SARS-CoV-2 nucleocapsid assembly inhibitors: Repurposing antiviral and antimicrobial drugs targeting nucleocapsid-RNA interaction

Debica Mukherjee[1,2], Upasana Ray*[1,2]

[1]CSIR-Indian Institute of Chemical Biology, 4, Raja S.C., Mullick Road, Jadavpur, Kolkata-700032, West Bengal, India.
[2]Academy of Scientific and Innovative Research (AcSIR), Ghaziabad- 201002, India

*Correspondence: ray.upasana@gmail.com
upasana.ray@iicb.res.in

Key words: SARS-CoV-2, nucleocapsid, assembly, drug repurposing

Abstract

SARS-CoV-2 pandemic has become a serious concern due to high transmission of this virus and unavailability of any definitive drugs yet in clinics. While novel antivirals are under investigation stage, scientists are also rigorously trying to use drug repurposing as an option to fight against this highly infectious novel coronavirus. Several drugs are under regular use for other diseases that are getting screened for their usability against SARS-CoV2. In this study we have targeted SARS-CoV-2 nucleocapsid assembly to shortlist FDA approved drugs that could be tested for inhibition of SARS-CoV-2 virus particles inside the host cell. We could shortlist seven antiviral and anti-microbial drugs. These showed good fit in docking studies inside the RNA binding cleft of the nucleocapsid protein. Also, these drugs have good lipophilic properties suggesting that they would enter the host cells. We propose that these shortlisted drugs could potentially compete out binding of viral RNA to nucleocapsid and thus inhibit successful virus assembly leading to poor virus progeny levels.

Introduction

SARS-CoV-2 pandemic has led to global search of therapeutics, either novel or repurposed from already existing drugs against other diseases. SARS-CoV-2 is an enveloped RNA virus that undergoes several steps of its life cycle within the host cell. Post entry the virus undergoes RNA translation, replication and virus assembly before new virus particles exit out of the host cells.

Starting from receptor binding on the host cell to virus exit out of the host cell, each of the steps are spearheaded by several viral structural and non-structural proteins.

Thus, functions of these viral proteins could be targeted to inhibit essential steps of the virus life cycle. SARS-CoV-2 spike protein, RdRp and helicase have been widely targeted for therapeutic interventions and drug repurposing. In this study we have targeted the nucleocapsid which assembles and packages the viral RNA inside. Inhibition of virus assembly and RNA packaging could lead to disruption in the virus life cycle and inhibit production of new virus particles thereby reducing the viral load post infection.

Methods:

Nucleocapsid substrate

Crystal structure of RNA binding N-terminal domain of nucleocapsid protein of SARS-CoV-2 was downloaded from Protein data bank (PDB) (1) (PDB entry: 6M3M). The 3D crystal structure consists of four equivalent chains of the RNA binding domains. As the nucleocapsid protein dimerizes during assembly, only two monomers (Chain A and B) were selected to retain the more native conformation for docking studies. The protein structure was converted to a supported file format (pdbqt) after removing the water molecules from the complex by AutoDock Tools 1.5.6 (3). Hydrogen atoms were added back to the side chains which retains an overall positive charge of the protein.

Ligand

In this study, we have screened an array of FDA approved anti-viral and anti-microbial drugs, which have not yet been reported against SARS-CoV2 as potential candidates. The nucleocapsid protein is only accessible in the intracellular environment. Hence, only those drugs have been selected as ligands which have significant lipophilic nature (Table 1). The 3D structure of drugs were downloaded in PDB format from Drug-bank (2). The ligand structure was converted to pdbqt format by AutoDock Tools 1.5.6 (3).

Molecular docking

All the protein-ligand docking experiments were done in Autodock vina software (v1.5.6) (4). We performed a blind docking, keeping the whole protein structure accessible for ligand

binding and the exhaustiveness value was 8. After docking the docked structures were visualized by Discovery Studio Visualizer v20.1.0.19295 (5) and PyMol software (6).

Results and discussion:

In this study FDA approved drugs have been screened for the purpose of drug repurposing against SARS-CoV-2 nucleocapsid assembly. For this virus to undergo successful nucleocapsid assembly, the nucleocapsid protein needs to interact/ bind with the viral RNA at the RNA binding cleft (Figure 1). This is a part of viral RNA packaging. Drugs that inhibit nucleocapsid-viral RNA binding might inhibit successful virus assembly inside the host cell. For a drug to act on virus assembly, it must be able to enter the host cells. Hence, we have picked drugs that showed lipophilic nature. Fifteen anti-viral compounds and fourteen anti-microbial compounds were screened.

After docking each drug, nine possible ligand binding possess were generated. Among those the best docked pose was selected with the higher binding affinity. According to docking score and number of non-covalent bonds made, seven anti-viral drugs (Figures 2-8) and seven anti-microbial drugs (Figures 9-15) were predicted to be the most suitable binding ligands for the nucleocapsid protein (Table 1).

Best docked ligands were selected by considering two parameters. Firstly, binding affinity that is less than -6 kcal/mol and the number of non-covalent bonds. Non- covalent bonds enable transient but strong binding between protein and ligand. Hence, the ligands which made a minimum of five non- covalent bonds were selected. Although, the value of binding energy for pentamidine is -5.6 kcal/mol, it was still selected as it interacts with seven non- covalent bonds.

The anti-viral compounds shortlisted have been in use either against HIV (Daclatasvir, tipranavir, fosamprenavir, etravirine, elvitegravir and rilapvirin) or HCMV (letermovir) (Table 1,2). These shortlisted antivirals show high affinity for binding with SARS-CoV-2 nucleocapsid. These ligands interact with the residues of the RNA binding cleft.

Our drug screening also revealed that some of the anti-microbial drugs also show significantly high binding ability with nucleocapsid protein of SARS-CoV-2 (Table 1,3) and thus these could be further tested for their possible antiviral activities in virus culture assays.

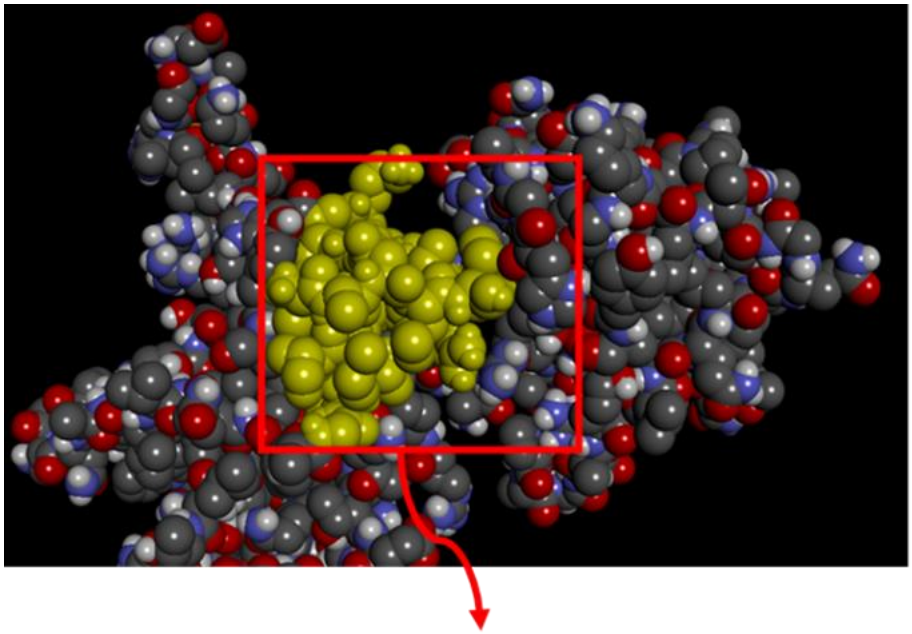

Figure1 : Dimerized nucleocapsid in globular display. Yellow highlighted residues interact with viral mRNA during packaging.

Amino acid residues in the binding pocket (lys66, Arg 69, Tyr124, Tyr110, Pro152, Pro 68, Arg 150, Ala 51, Pro 68) are maximally involved in the interaction with the shortlisted ligands. Since the screened drug candidates are docking into the RNA binding cleft, we hypothesize that they might potentially compete out the viral RNA and thus inhibit nucleocapsid assembly.

The flexibility of a molecule and presence of water molecule in cellular environment can significantly alter the interaction properties. Thus, all the screened drug molecules need further validations in virus assembly assay systems and virus culture models.

A

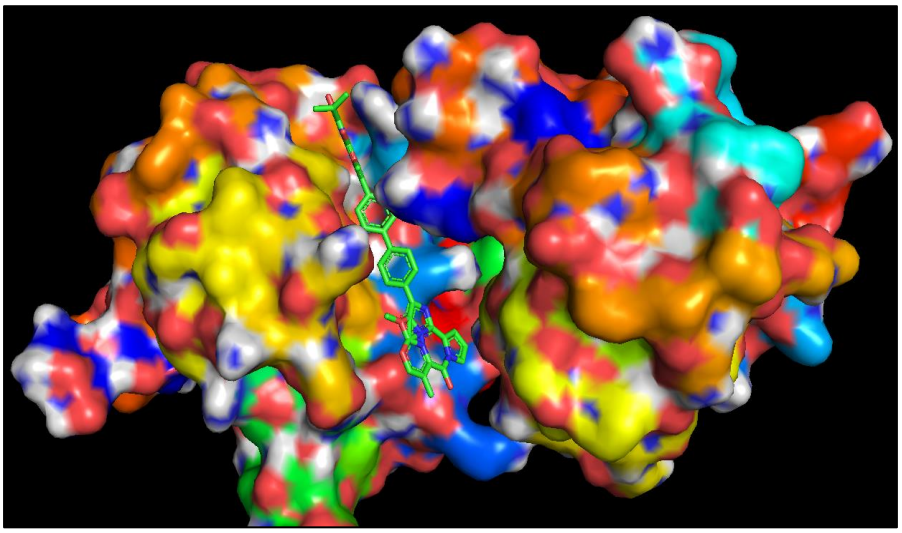

B

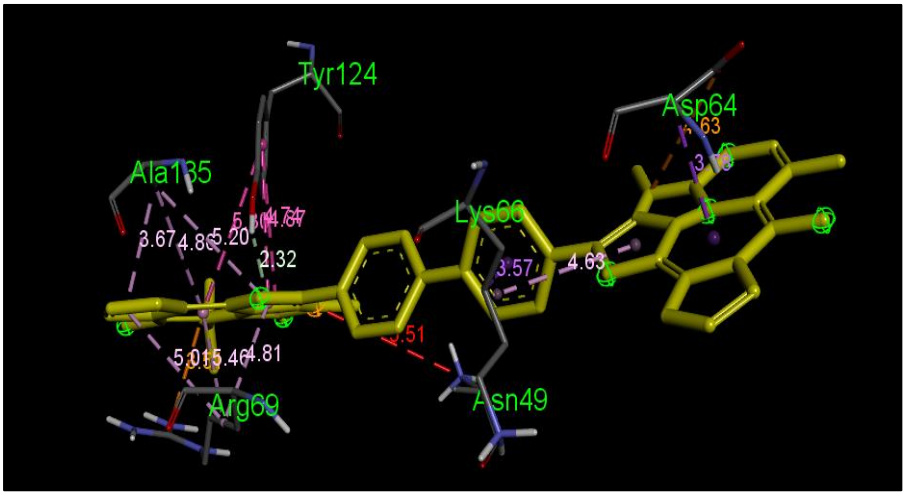

C

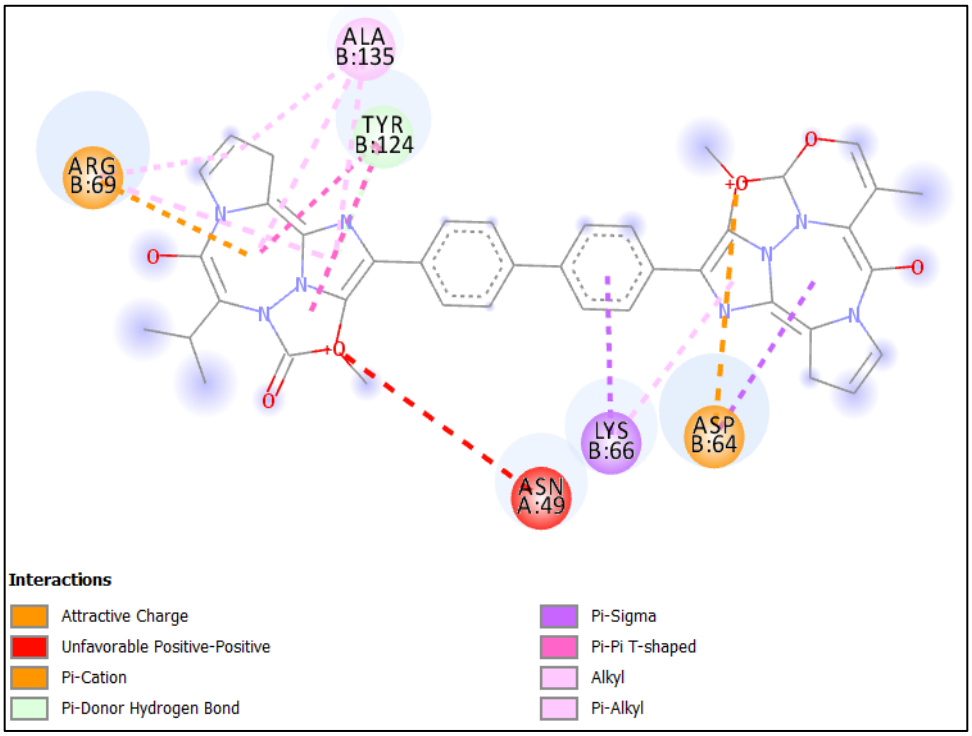

Figure 2: **Daclatasvir docked in N-terminal domain of SARS-CoV2 nucleocapsid protein**. A. Best fit 3D binding pocket of Daclatasvir. B. Interacting amino acid side chains with bond lengths indicated. C. Two-dimensional display of interaction

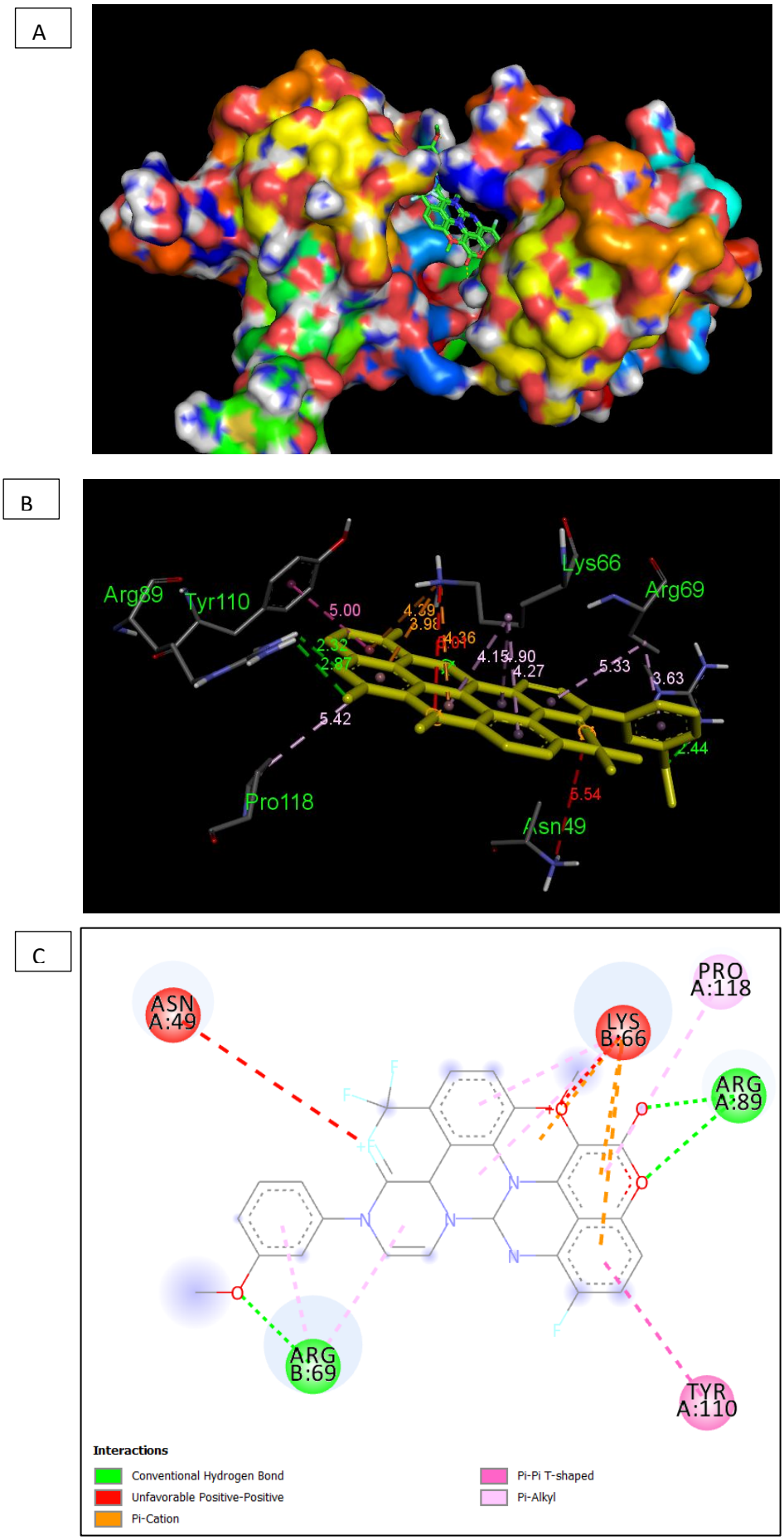

Figure 3: Letermovir docked in N-terminal domain of SARS-CoV2 nucleocapsid protein. A. Best fit 3D binding pocket of Letermovir. B. Interacting amino acid side chains with bond lengths indicated. C. Two-dimensional display of interaction

A

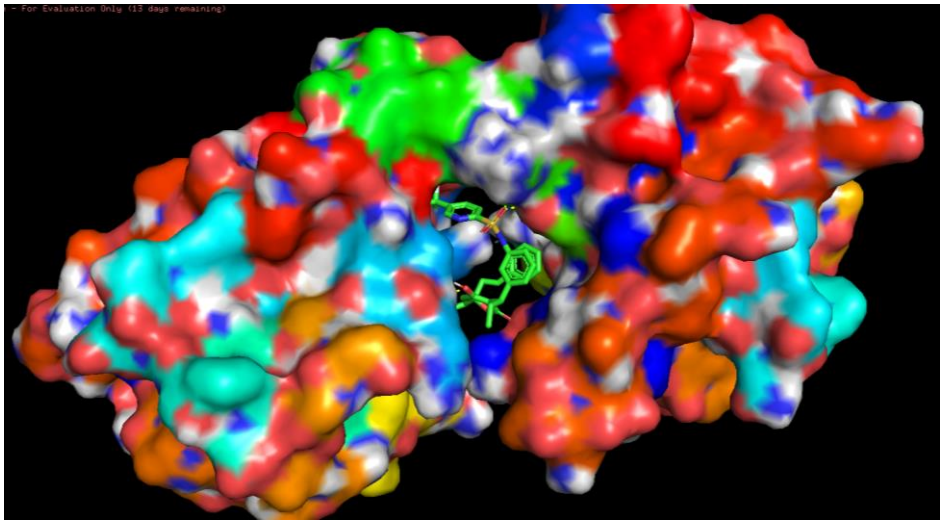

B

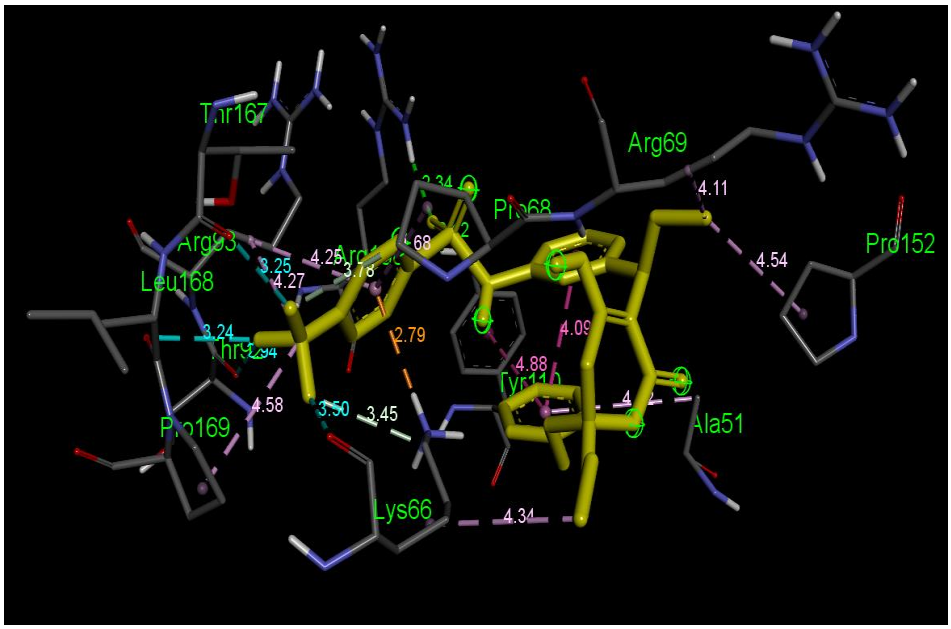

C

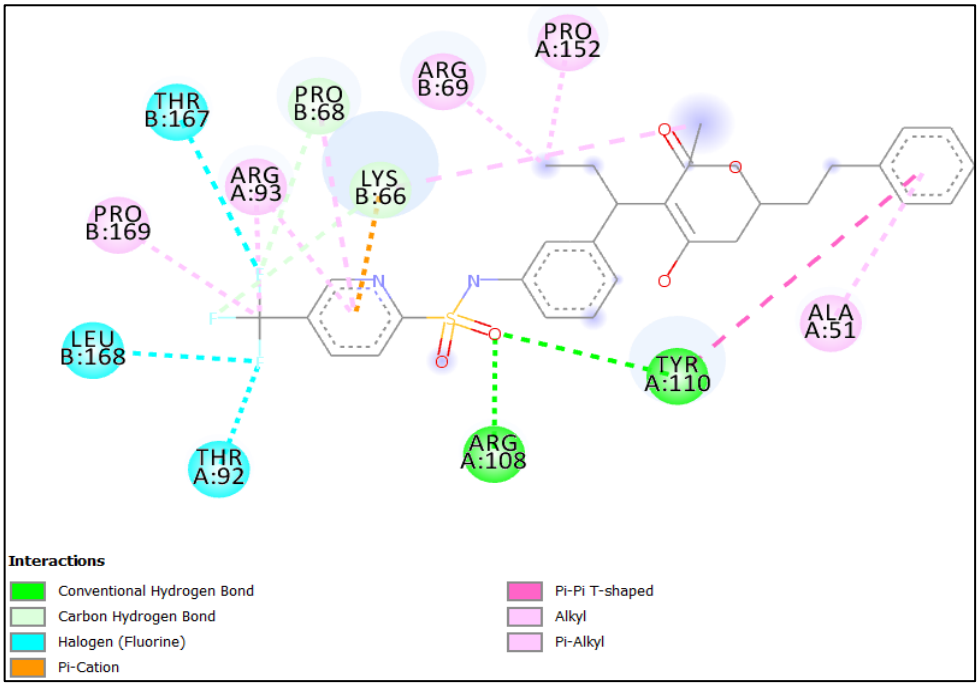

Figure 4: Tipranavir docked in N-terminal domain of SARS-CoV2 nucleocapsid protein. A. Best fit 3D binding pocket of Tipranavir. B. Interacting amino acid side chains with bond lengths indicated. C. Two-dimensional display of interaction

A

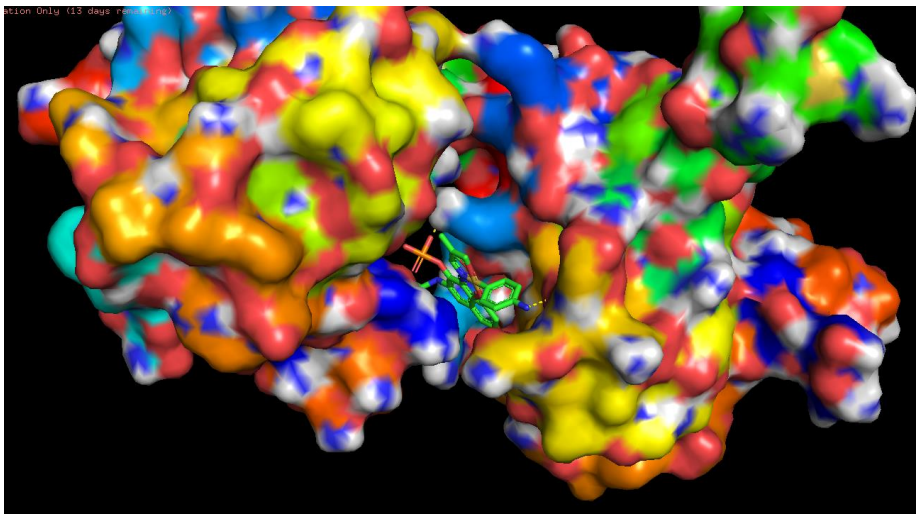

B

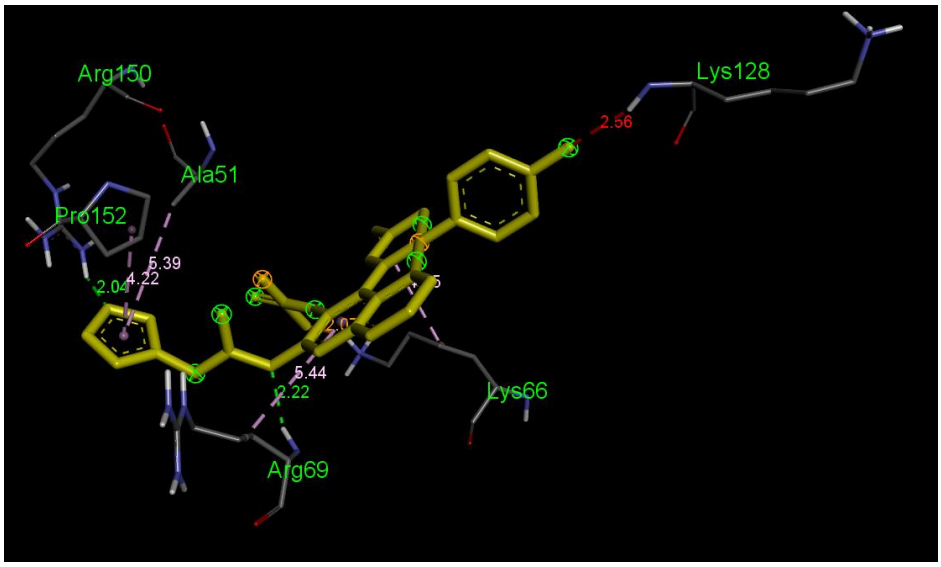

C

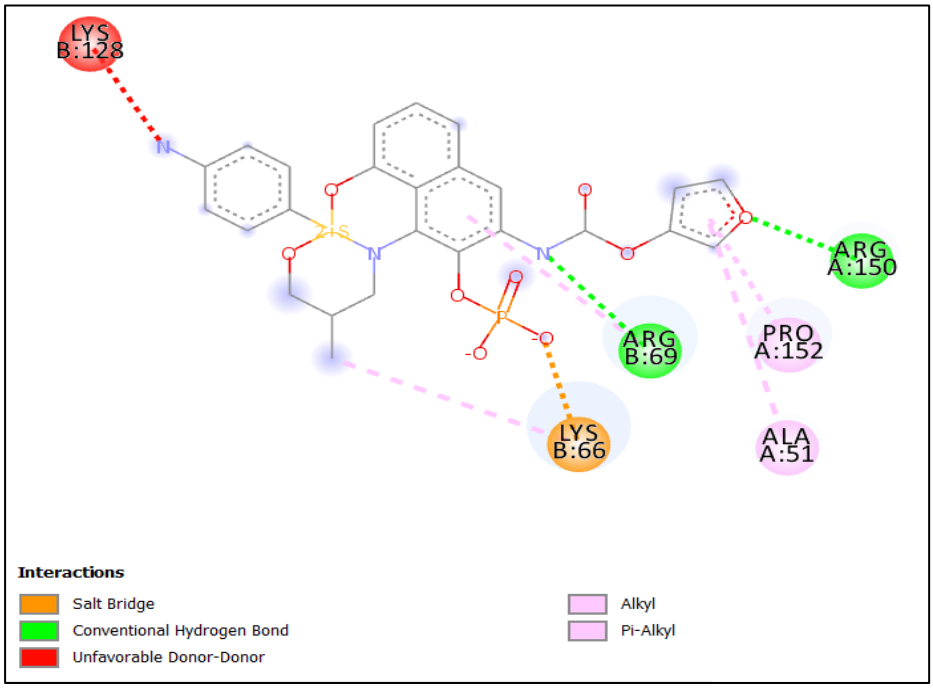

Figure 5: Fosamprenavir docked in N-terminal domain of SARS-CoV2 nucleocapsid protein. A. Best fit 3D binding pocket of Fosamprenavir. B. Interacting amino acid side chains with bond lengths indicated. C. Two-dimensional display of interaction.

A

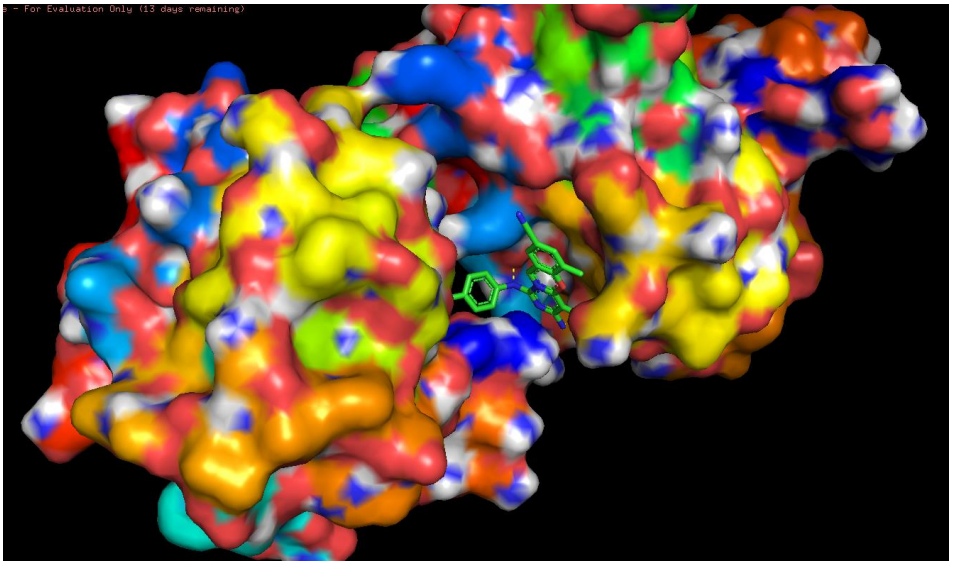

B

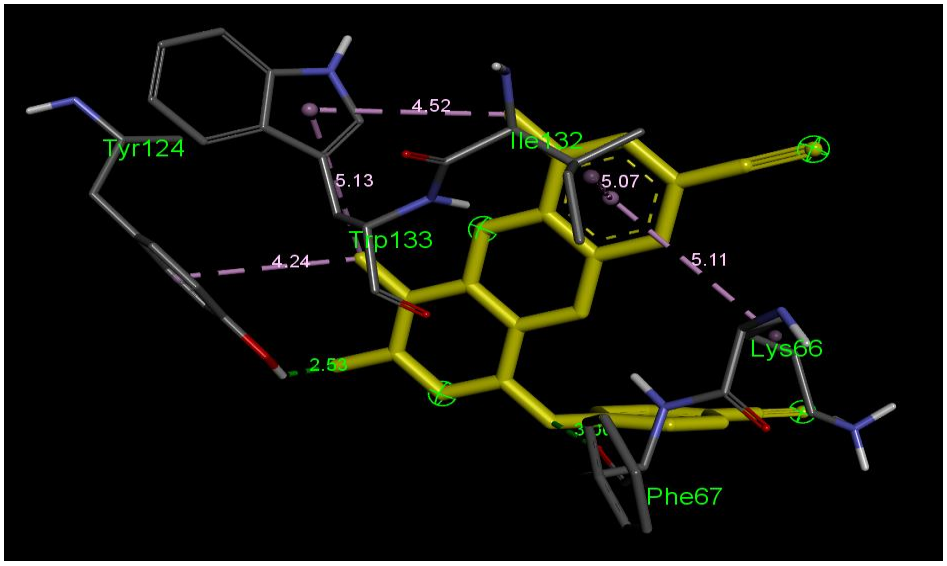

C

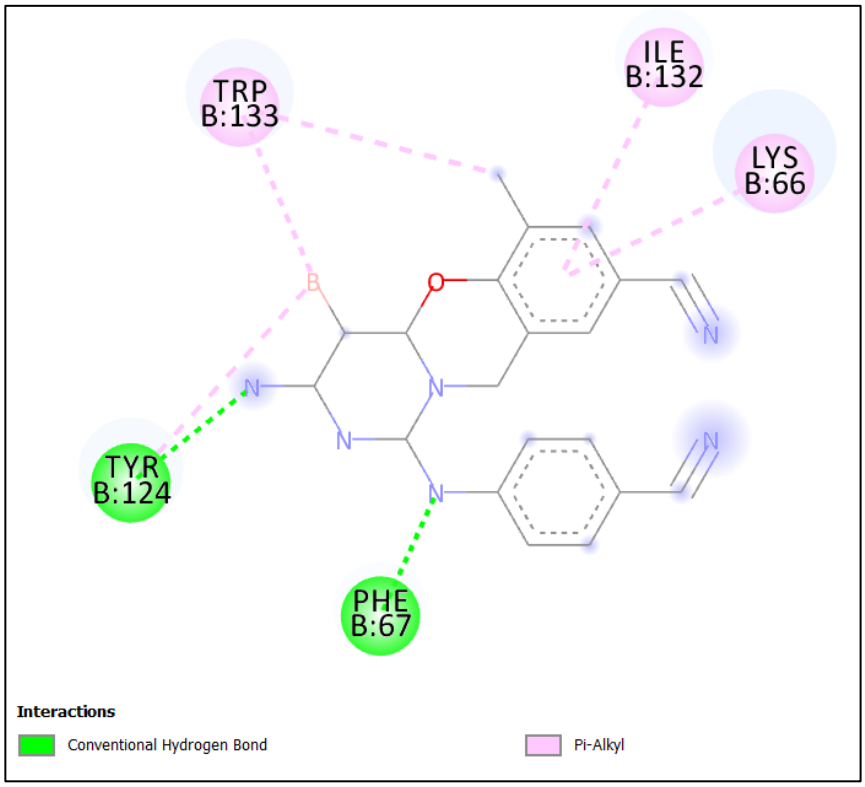

Figure 6: Etravirine docked in N-terminal domain of SARS-CoV2 nucleocapsid protein. A. Best fit 3D binding pocket of Etravirine. B. Interacting amino acid side chains with bond lengths indicated. C. Two-dimensional display of interaction

A

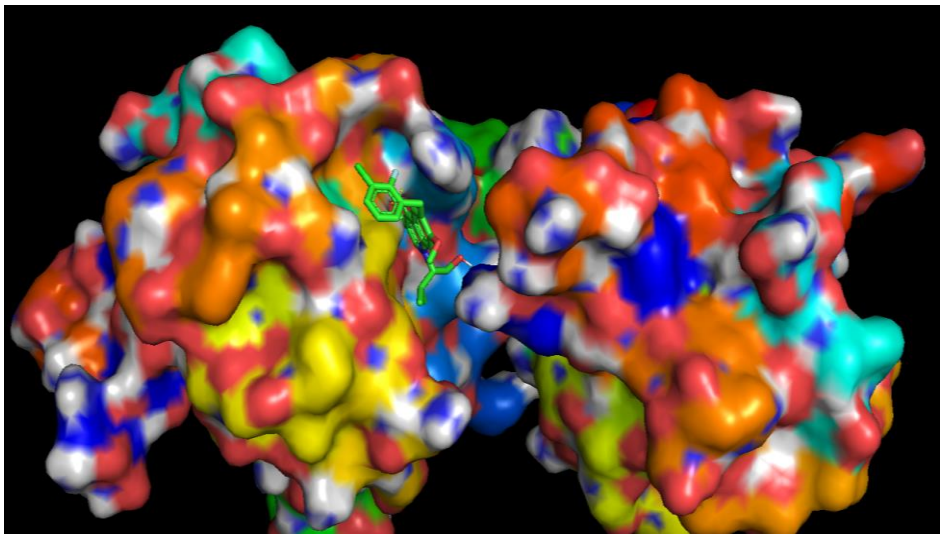

B

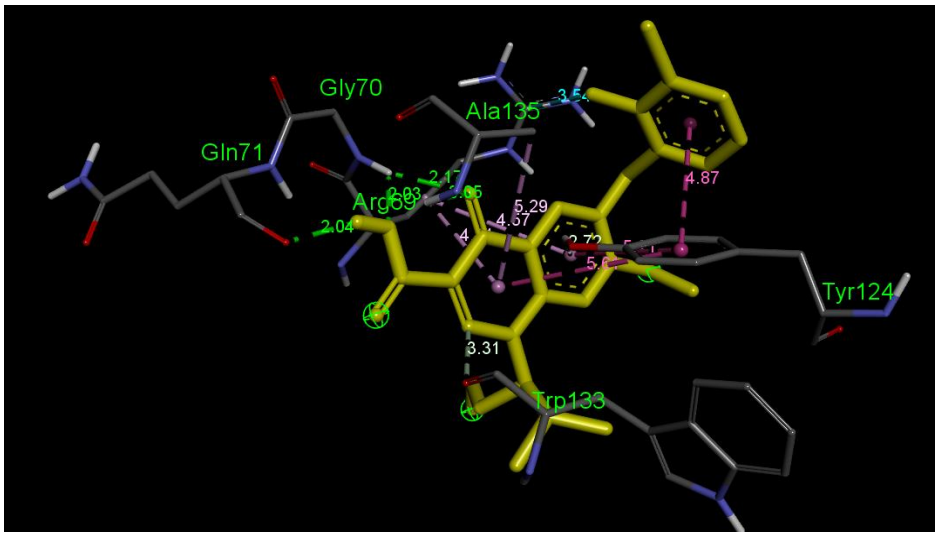

C

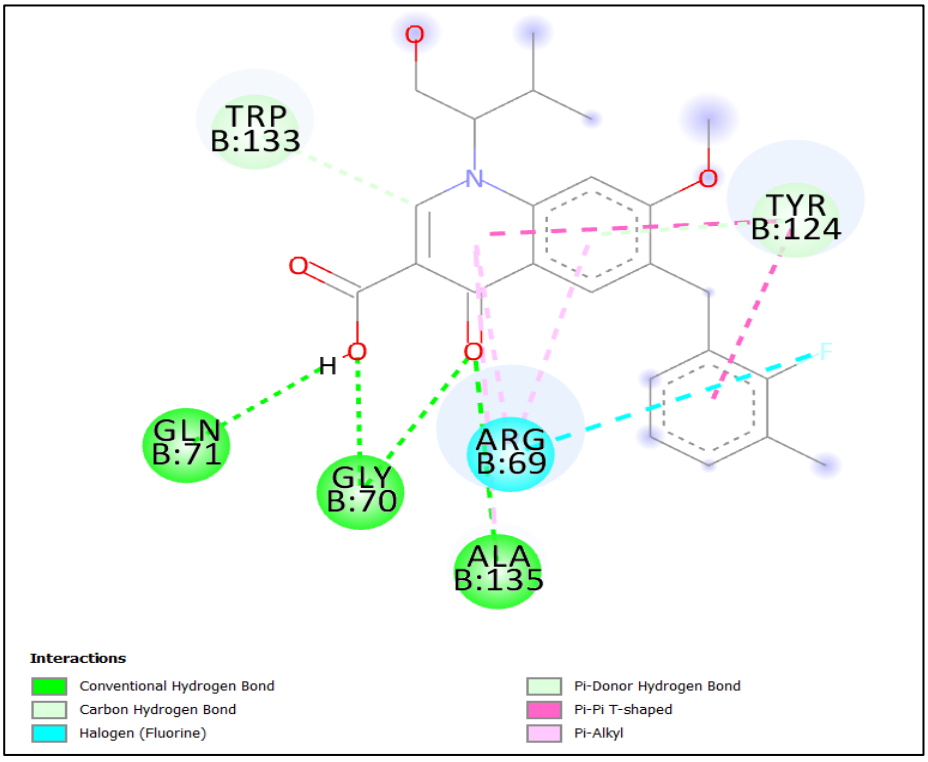

Figure 7: Elvitegravir docked in N-terminal domain of SARS-CoV2 nucleocapsid protein. A. Best fit 3D binding pocket of Elvitegravir. B. Interacting amino acid side chains with bond lengths indicated. C. Two-dimensional display of interaction

A

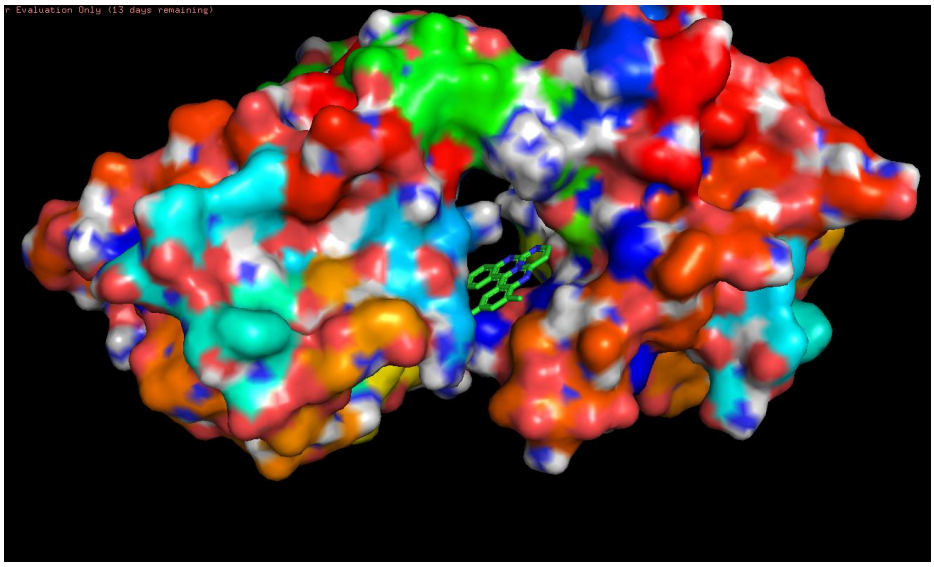

B

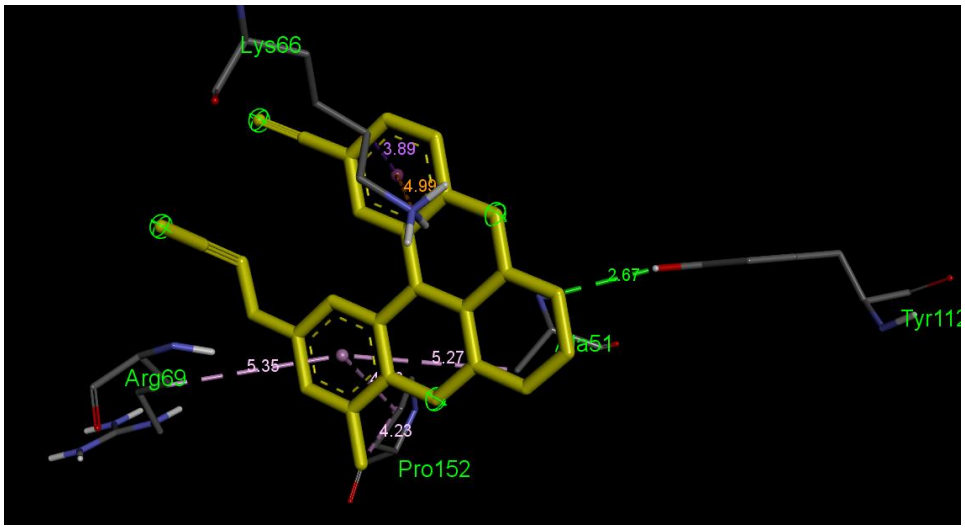

C

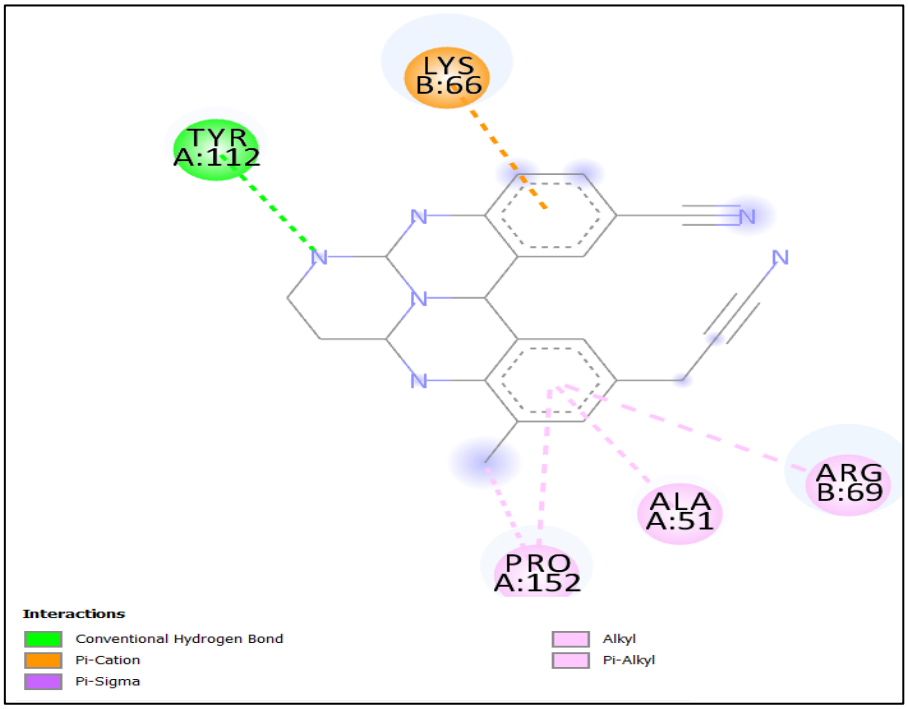

Figure 8: Rilpivirine docked in N-terminal domain of SARS-CoV2 nucleocapsid protein. A. Best fit 3D binding pocket of Rilpivirine. B. Interacting amino acid side chains with bond lengths indicated. C. Two-Dimensional display of interaction

A

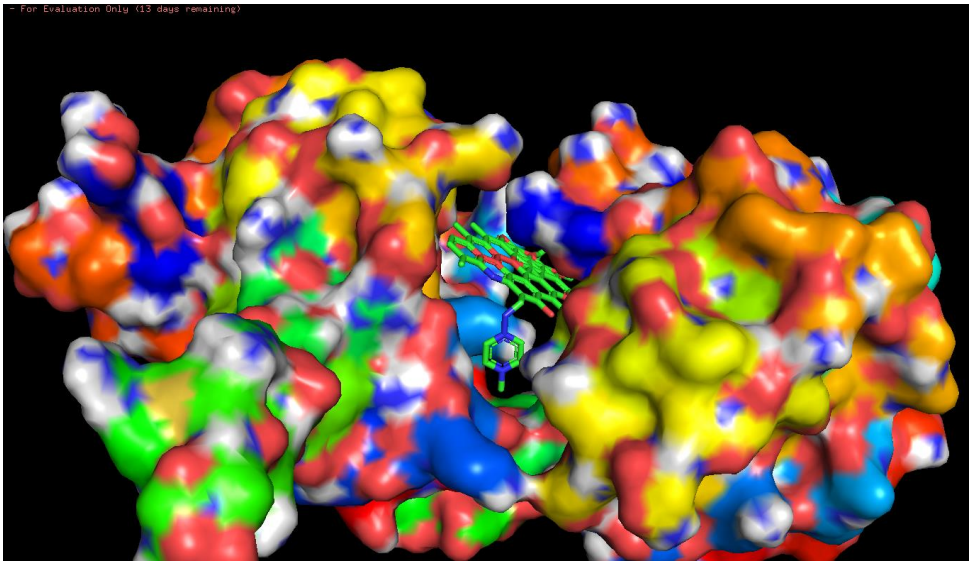

B

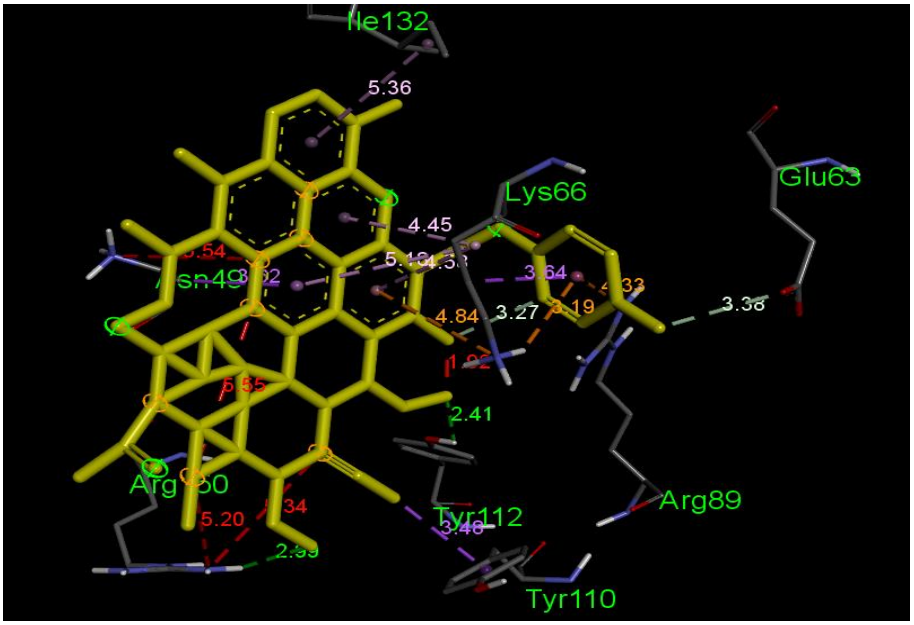

C

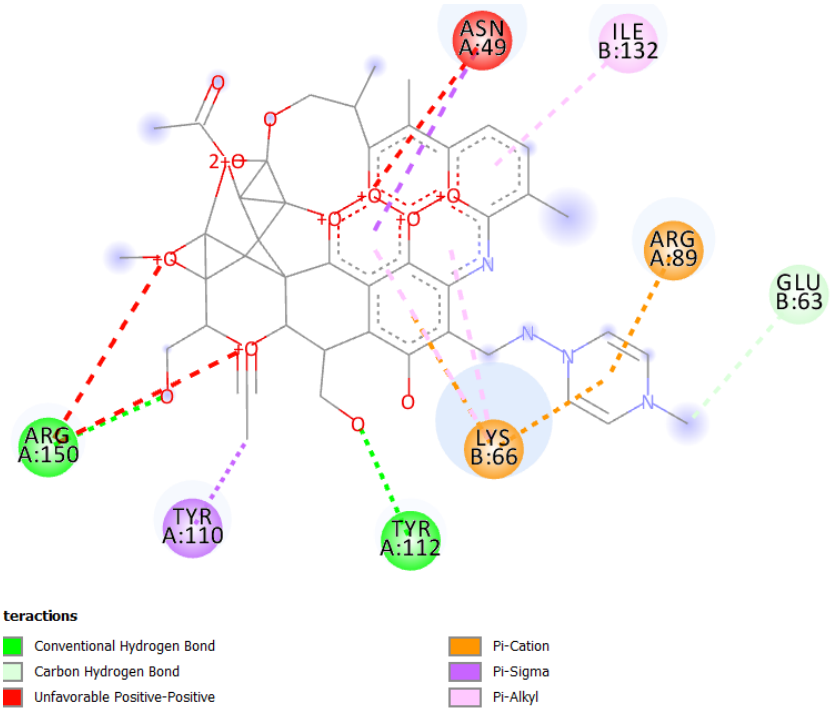

Figure 9: Rifampicin docked in N-terminal domain of SARS-CoV2 nucleocapsid protein. A. Best fit 3D binding pocket of Rifampicin. B. Interacting amino acid side chains with bond lengths indicated. C. Two- Dimensional display of interaction.

A

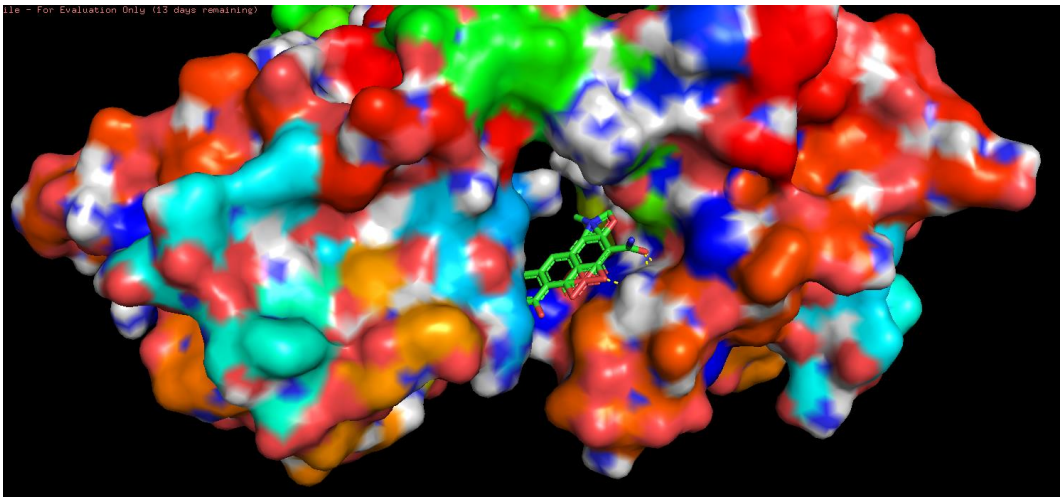

B

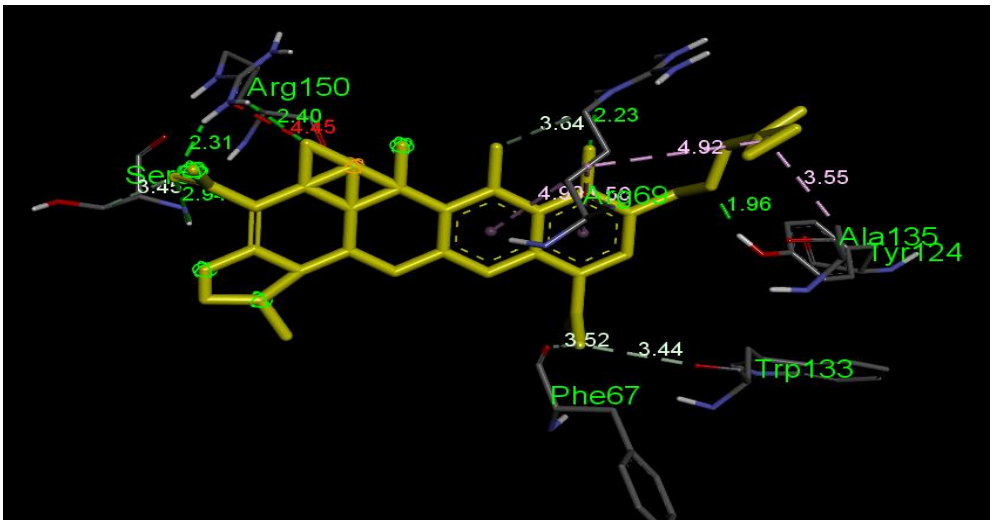

C

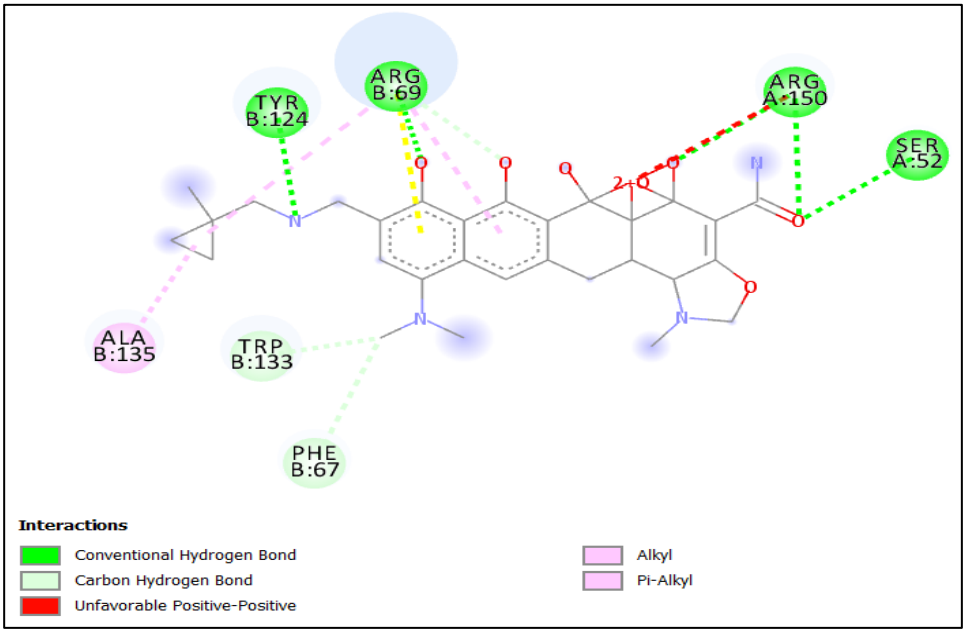

Figure 10: Omadacycline docked in N-terminal domain of SARS-CoV2 nucleocapsid protein. A. Best fit 3D binding pocket of Omadacycline. B. Interacting amino acid side chains with bond lengths indicated. C. Two-dimensional display of interaction.

A

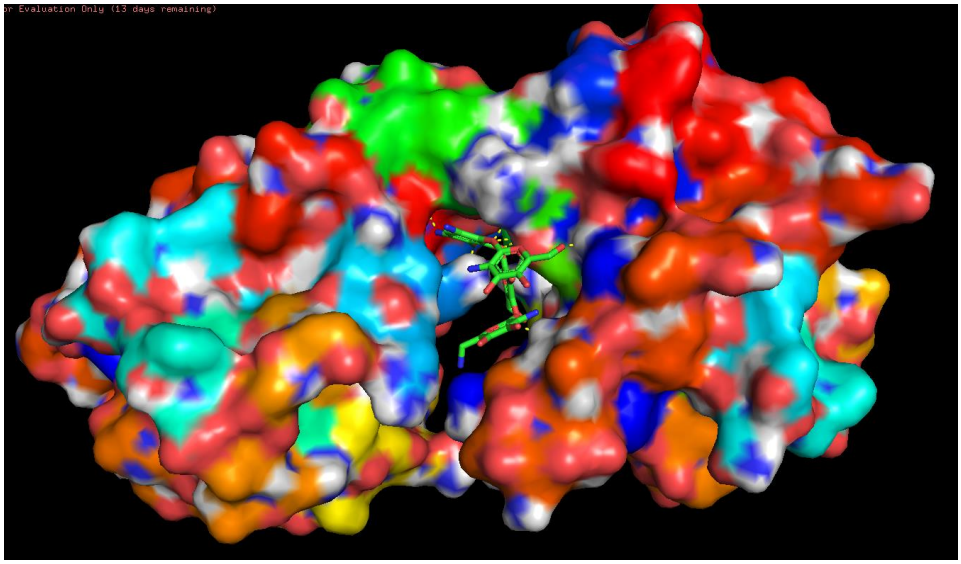

B

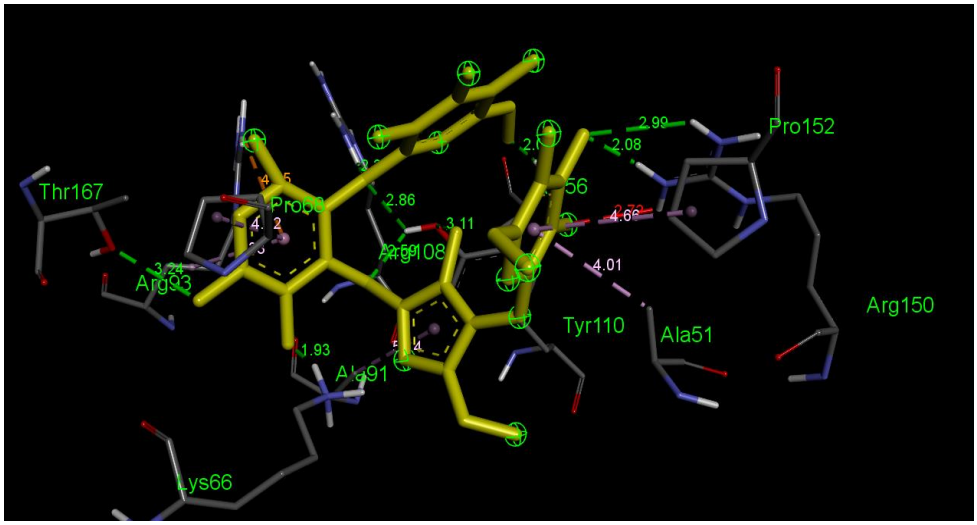

C

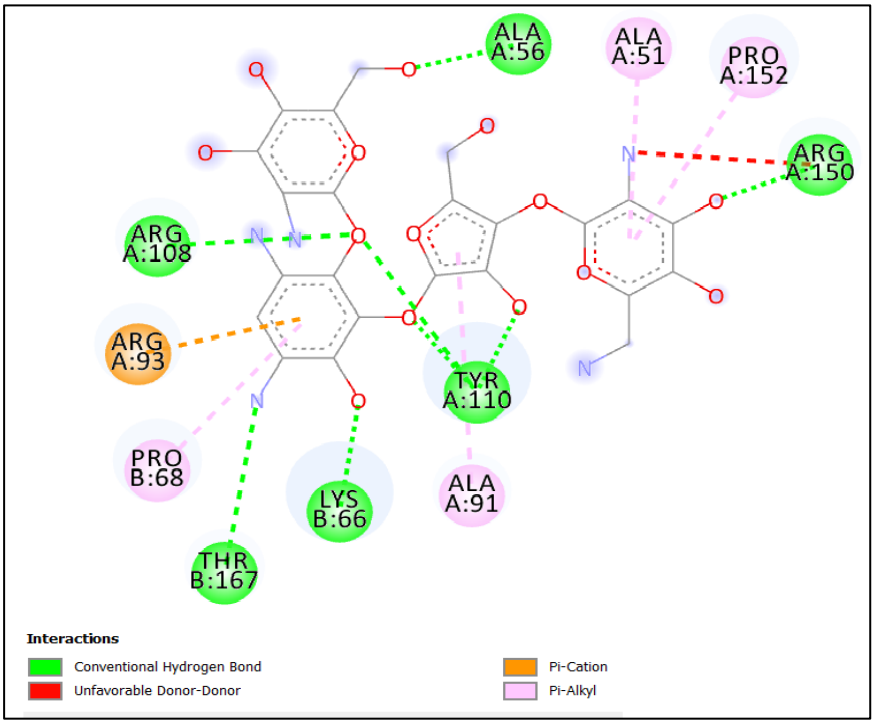

Figure 11: Paromomycin docked in N-terminal domain of SARS-CoV2 nucleocapsid protein. A. Best fit 3D binding pocket of Paromomycin. B. Interacting amino acid side chains with bond lengths indicated. C. Two- dimensional display of interaction.

A

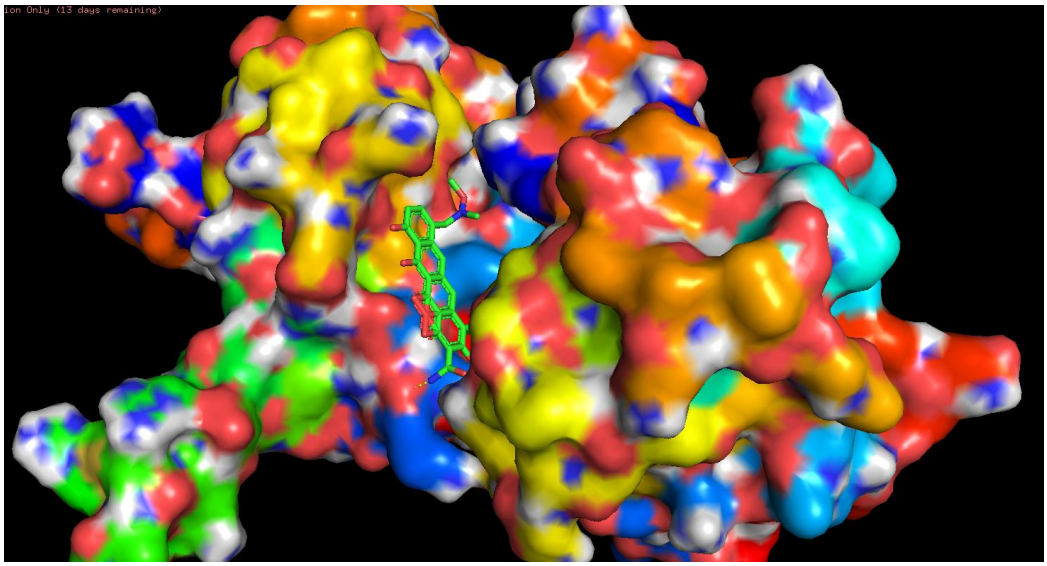

B

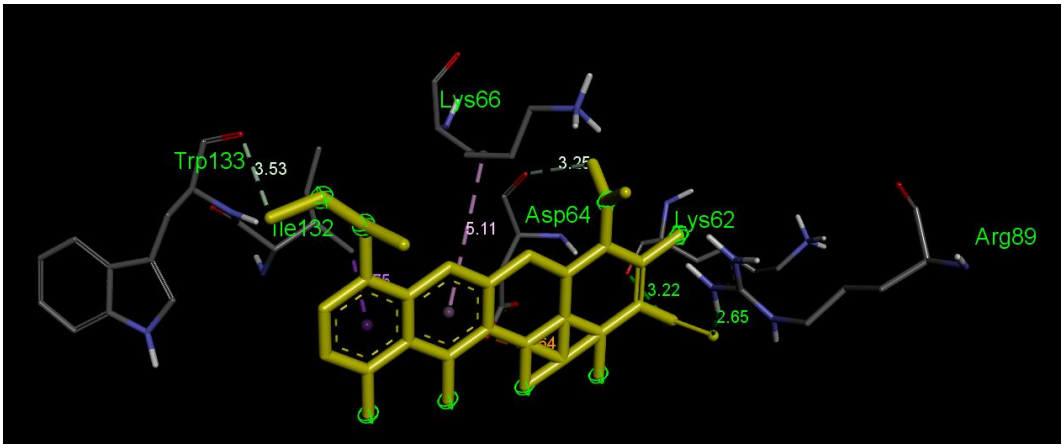

C

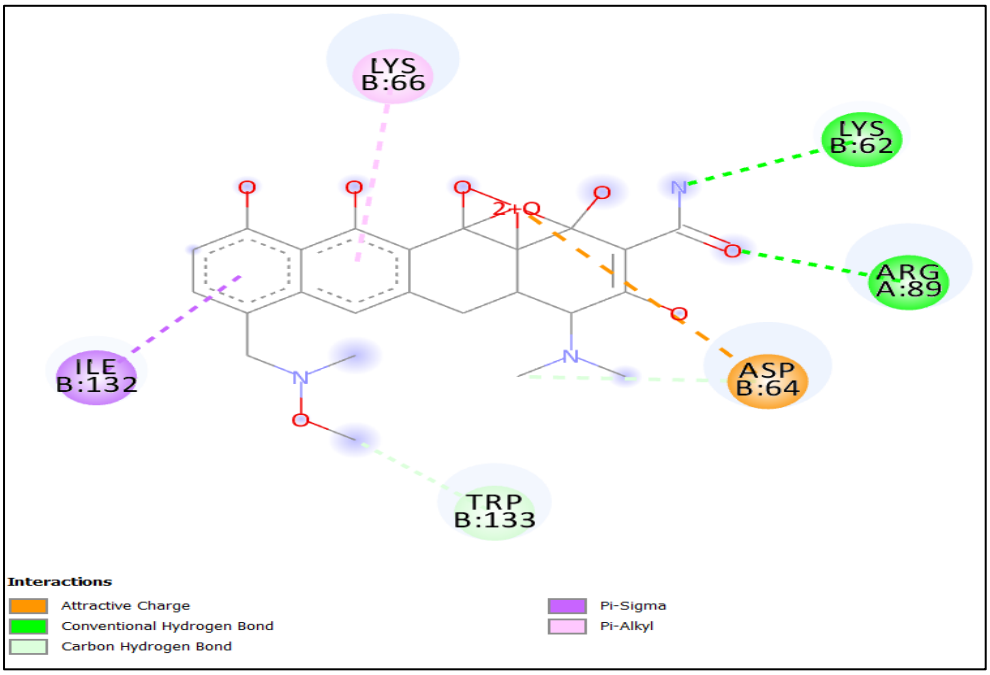

Figure 12: Sarecycline docked in N-terminal domain of SARS-CoV2 nucleocapsid protein. A. Best fit 3D binding pocket of Sarecycline. B. Interacting amino acid side chains with bond lengths indicated. C. Two- dimensional display of interaction

A

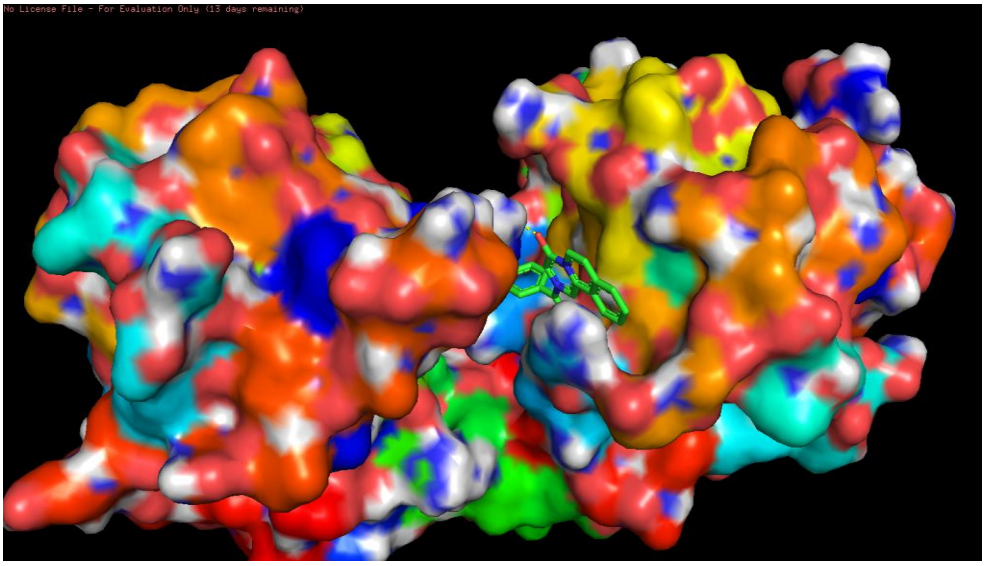

B

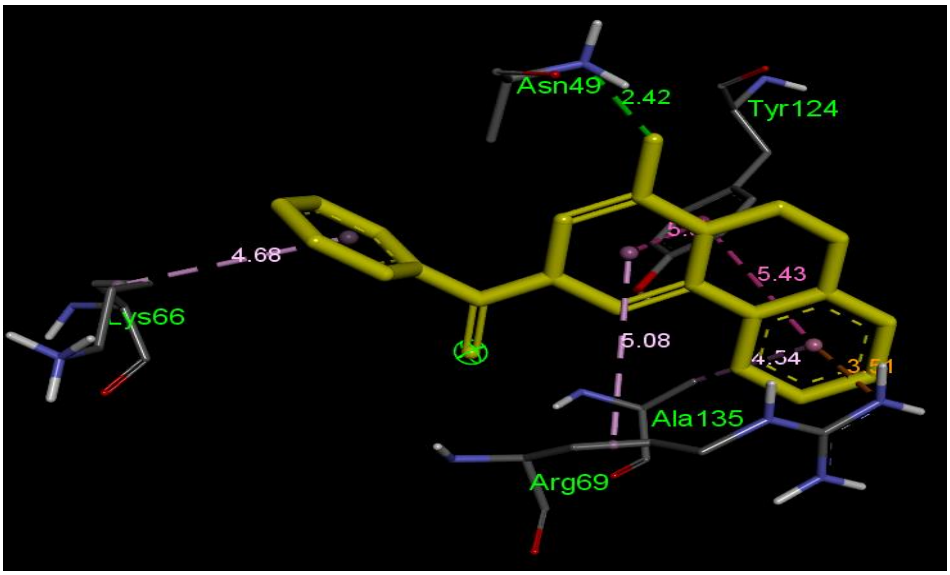

C

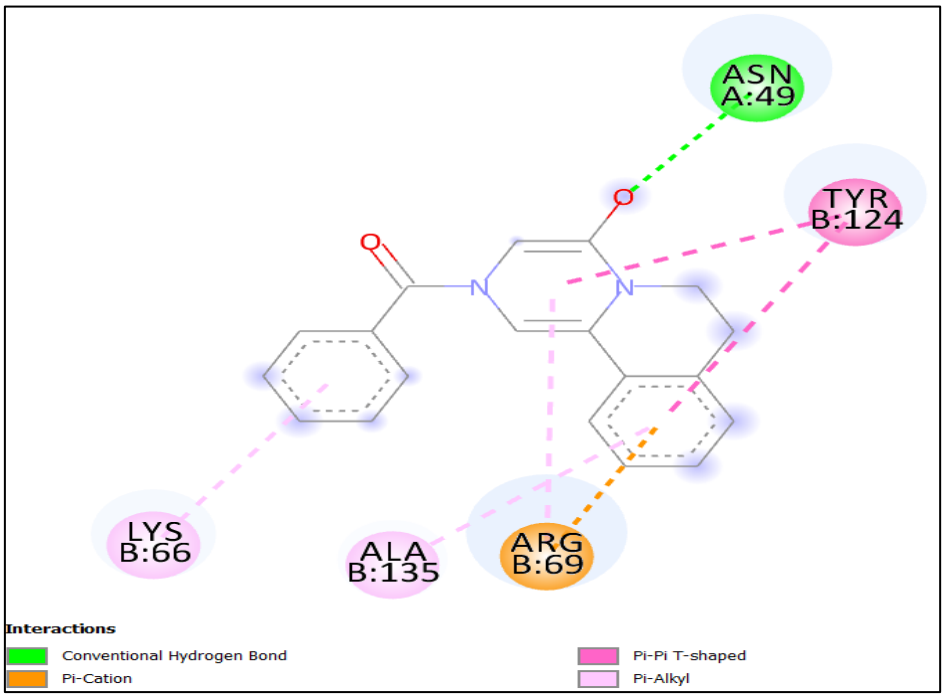

Figure 13: Praziquantel docked in N-terminal domain of SARS-CoV2 nucleocapsid protein. A. Best fit 3D binding pocket of Praziquantel. B. Interacting amino acid side chains with bond lengths indicated. C. Two- dimensional display of interaction

A

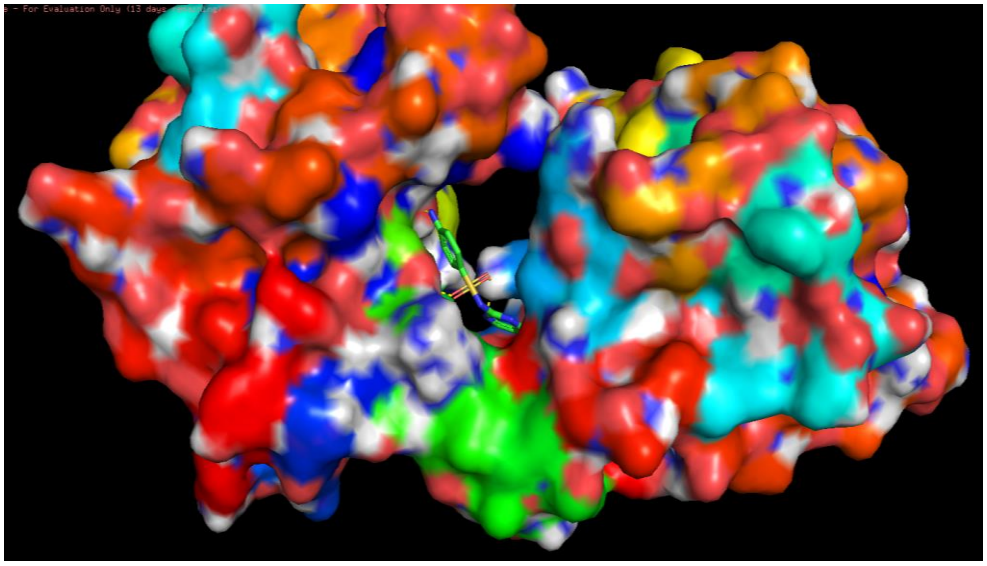

B

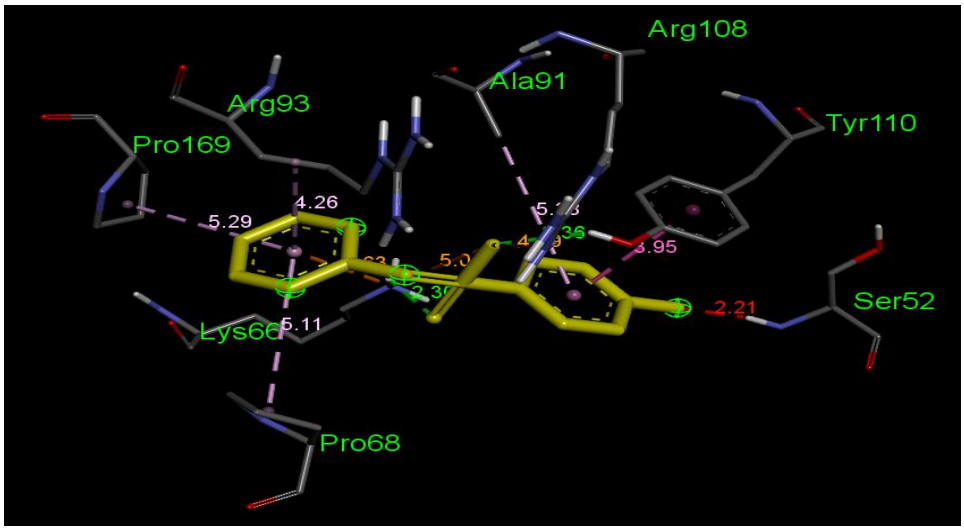

C

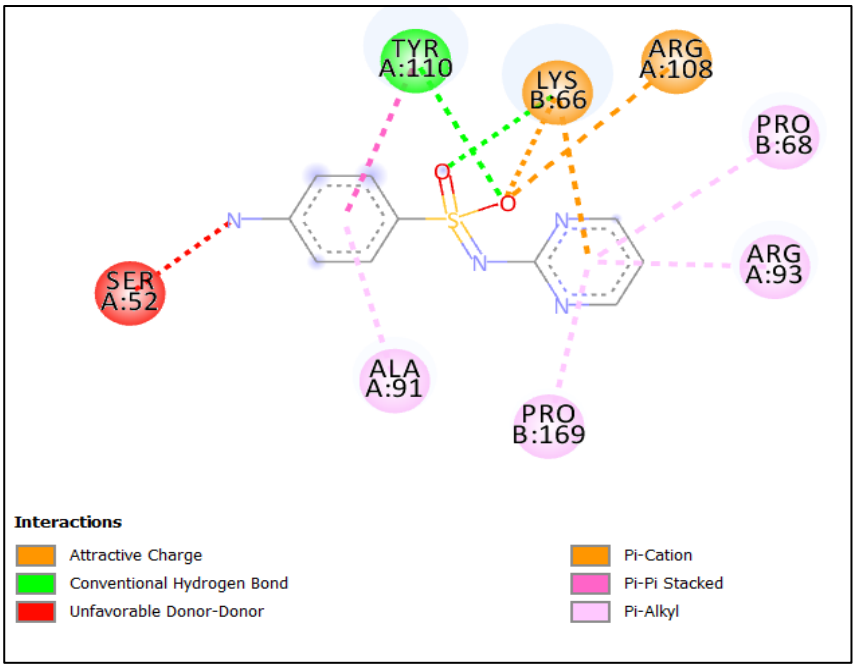

Figure 14: Sulfadiazine docked in N-terminal domain of SARS-CoV2 nucleocapsid protein. A. Best fit 3D binding pocket of Sulfadiazine. B. Interacting amino acid side chains with bond lengths indicated. C. Two-dimensional display of interaction.

A

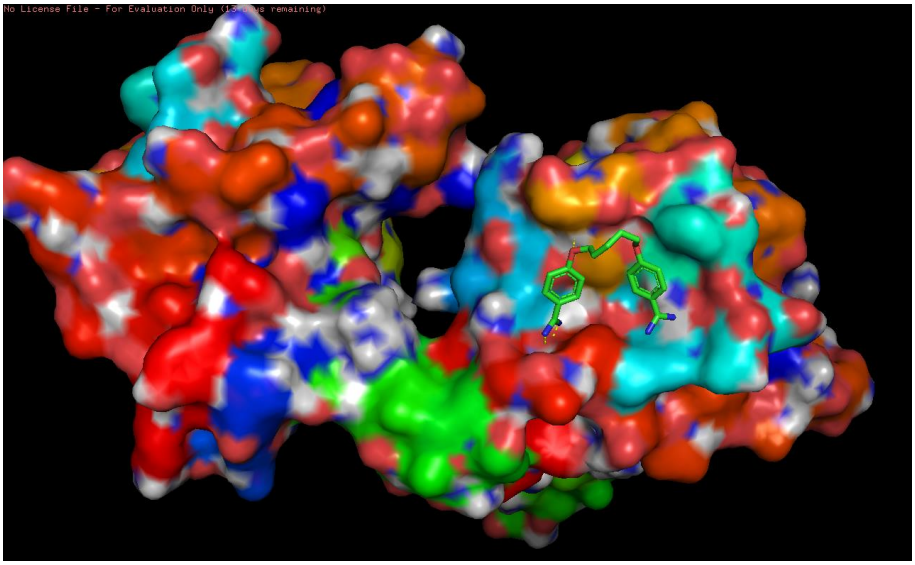

B

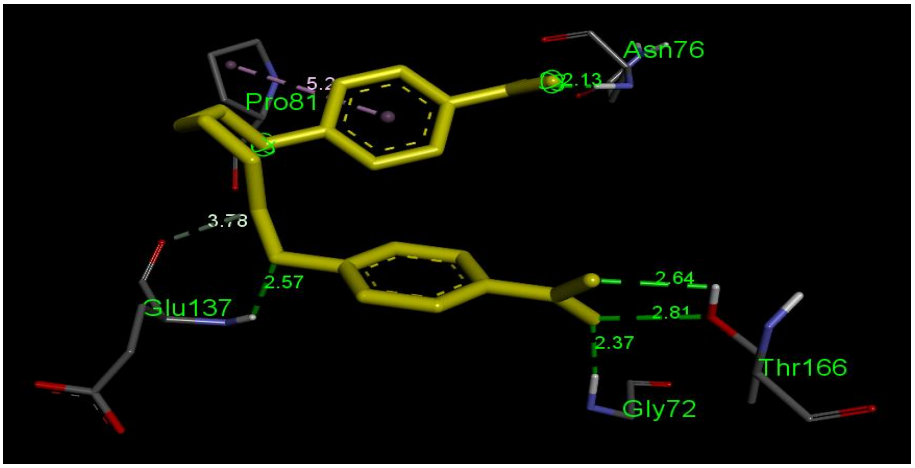

C

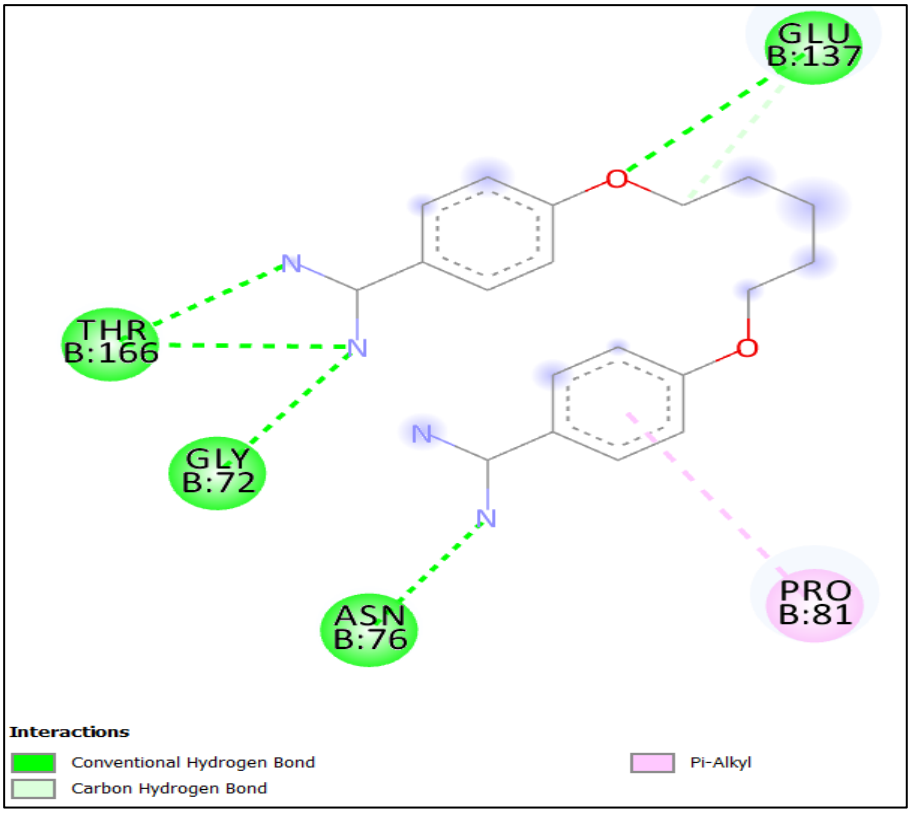

Figure 15: Pentamidine docked in N-terminal domain of SARS-CoV2 nucleocapsid protein. A. Best fit 3D binding pocket of Pentamidine. B. Interacting amino acid side chains with bond lengths indicated. C. Two-dimensional display of interaction.

Type of drug	Name of drug (Drug Bank ID)	Lipophilicity (logP)	Binding affinity (kcal/Mol)	Types of bond	Interacting amino acids	Bond length (Å)
Anti-viral	**Daclatasvir** (DB09102)	4.67	-10.9	Pi-sigma Pi-cation Pi-alkyl Pi-Pi T shaped	Lys 66 (B) Asp 64 (B) Arg 69 (B) Ala 135 (B) (3) Lys 66 (B) Tyr 124 (B) (3)	3.5 3.7 3.5 5.2, 4.8, 3.6 4.6 4.8, 5.3, 4.7
Anti-viral	**Letermovir** (DB12070)	4.58	-9.7	H-bond Pi-cation Pi-alkyl Pi-Pi T shaped	Arg 69 (B) Arg 89 (A) (2) Lys 66 (B) (3) Pro 118 (A) Tyr 110 (A)	2.4 2.3, 2.8 4.2, 4.9, 4.1 5.4 5.0
Anti-viral	**Tipranavir** (DB00932)	6.29	-8.1	H-bond Halogen bond Pi-alkyl Pi-cation C-H bond Pi-Pi T shaped	Arg 108 (A) Tyr 110 (A) Thr 167 (B) Leu 168 (B) Thr 92 (A) Pro 169 (B) Arg 93 (A) (2) Arg 69 (B) Pro 152 (A) Pro 68 (B) Lys 66 (B) Ala 51 (A) Lys 66 (B) Pro 68 (B) Lys 66 (B) Tyr 110 (A)	2.3 2.1 3.2 3.2 2.9 4.5 4.2, 4.2 4.1 4.5 4.6 4.3 4.9 2.7 3.7 3.4 4.8
Anti-viral	**Fosamprenavir** (DB01319)	0.84	-7.8	H-bond Pi-alkyl Salt Bridge	Arg 69 (B) Arg 150 (A) Pro 152 (A) Ala 51 (A) Lys 66 (B) Arg 69 (B) Lys 66 (B)	2.2 2.04 4.22 5.32 4.9 5.4 2.0
Anti-viral	**Etravirine** (DB06414)	3.6	-7.6	H-bond	Tyr 124 (B) Phe 67 (B)	2.5 3.0

				Pi-alkyl	Trp 133 (B) (2) Ile 132 (B) Lys 66 (B) Tyr 124 (B)	4.5, 5.1 5.0 5.1 4.2
Anti-viral	**Elvitegravir** (DB09101)	3.66	-7.5	H-bond Pi-alkyl Halogen bond C-H bond Pi-Pi T shaped	Gln 71 (B) Gly 70 (B) (2) Ala 135 (B) Ala135 (B) Arg 69 (B) (2) Arg 69 (B) Trp 133 (B) Tyr 124 (B) (3)	2.4 2.1, 2.0 3.0 5.2 4.5, 4.3 3.5 3.3 4.8, 5.6, 5.2
Anti-viral	**Rilpivirine** (DB08864)	3.8	-7.3	H-bond Pi-cation Pi-alkyl Pi-sigma	Tyr 112 (A) Lys 66 (B) Pro 152 (A) (2) Ala 51 (A) Arg 69 (B) Lys 66 (B)	2.6 4.9 4.6, 4.2 5.2 5.3 3.8
Anti-bacterial	**Rifampicin** (DB01045)	3.85	-11.9	H-bond C-H bond Pi-cation Pi-sigma Pi-alkyl	Arg 150 (A) Tyr 112 (A) Glu 63 (B) Lys 66 (B) (2) Arg 89 (A) Tyr 110 (A) Asn 49 (A) Ile 32 (B)	2.9 2.4 3.3 4.8, 3.1 4.3 3.4 3.6 5.3
Anti-bacterial	**Omadacycline** (DB12455)	0.94	-9.0	H-bond C-H bond Pi-alkyl 	Tyr 124 (B) Arg 69 (B) Arg 150 (A) (2) Ser 52 (A) Trp 133 (B) Phe 67 (B) Arg 69 (B) (3) Ala 135 (B)	1.9 2.2 2.3, 2.4 2.9 3.4 3.5 4.9,4.5,4.9 3.5
Anti-bacterial	**Paromomycin** (DB01421)	2.9	-8.1	H-bond 	Arg 108 (A) Thr 167 (B) Lys 66 (B) Tyr 110 (B) (3) Arg 150 (A) (2) Ala 56 (A)	2.3 3.2 1.9 2.8, 3.1, 2.9 2.0, 2.9 2.0

				Pi-cation	Arg 93 (A)	4.9
				Pi-alkyl	Pro 68 (B) Ala 51 (A) Pro 152 (A) Ala 91 (A)	4.7 4.0 4.6 5.1
Anti-bacterial	**Sarecycline** (DB12035)	0.17	-7.3	H-bond Attractive charge C-H bond Pi-sigma Pi-alkyl	Lys 66 (B) Arg 89 (A) Asp 64 (B) Asp 64 (B) Trp 133 (B) Ile 132 (B) Lys 66 (B)	3.2 2.6 3.6 3.2 3.5 3.7 5.1
Anti-parasitic	**Praziquantel** (DB01058)	2.42	-6.7	H-bond Pi-Pi T shaped Pi-cation Pi-alkyl	Asn 49 (A) Tyr 124 (B) (2) Arg 69 (B) Arg 69 (B) Ala 135 (A) Lys 66 (B)	2.4 5.5, 5.4 3.5 5.0 4.5 4.6
Anti-bacterial	**Sulfadiazine** (DB00359)	0.25	-6.2	H-bond Pi-alkyl Attractive charge Pi-cation	Tyr 110 (A) Lys 66 (B) Pro 68 (B) Arg 93 (A) Ala 91 (A) Pro 169 (B) Lys 66 (B) Arg 108 (A) Lys 66 (B)	2.3 2.3 5.1 4.2 5.3 5.2 5.0 4.3 3.6
Anti-protozoa	**Pentamidine** (DB00738)	1.32	-5.6	H-bond C-H bond Pi-alkyl	Thr 166 (B) (2) Gly 72 (B) Asn 76 (B) Glu 137 (B) Glu 137 (B) Pro 81 (B)	2.6, 2.8 2.3 2.1 2.5 3.7 5.2

Table1: Details of shortlisted drugs

Name of drug	Approved against	Mode of Action	Drug bank ID
Letermovir	HCMV	DNA terminase complex of human cytomegalovirus is required to cut the DNA before virus assembly. Letermovir blocks the DNA terminase complex thus inhibiting DNA processing.	DB12070
Daclatasvir	HCV	Daclatasvir binds to the N-terminus of the D1 domain of NS5A of hepatitis C virus This domain interacts with various host cell proteins and membranes during replication complex formation.	DBSALT001166
Elvitegravir	HIV	Integrase enzyme of HIV incorporates viral Genome into the host genome. Elvitegravir inhibits the strand transfer by integrase in HIV-1.	DB09101
Rilpivirine	HIV	Rilpivirine binds to reverse transcriptase (RT) enzyme of HIV-1 and blocks replication in a non-competitive manner.	DB08864
Etravirine	HIV	Etravirine directly binds and inhibits reverse transcriptase enzyme activity HIV -1	DB06414
Tipranavir	HIV	Tipranavir inhibit the formation of functional viral protein by binding to viral protease.	DB00932
Fosamprenavir	HIV	Fosamprenavir is hydrolyzed to amprenavir by intracellular phosphatases. Fosamprenavir inhibits HIV-1 protease and thus blocks viral Gag and Gag-pol polyprotein processing.	DB01319

Table2: Mode of action of shortlisted anti-viral drugs

Name of drug	Approved against	Mode of Action	Drug bank ID
Paromomycin	Enteric bacteria	Paromomycin inhibit bacterial protein synthesis by binding to the 16S ribosomal RNA	DB01421
Rifampicin	Bacteria	Rifampin blocks RNA synthesis in bacterial cells by inhibition of DNA- dependent RNA polymerase.	DB01045
Sulfadiazine	Bacteria	Dihydropteroate synthetase enzyme of required for folic acid biosynthesis. Sulfadiazine inhibits this enzyme and folic acid synthesis	DB00359
Sarecycline	Bacteria	Sarecycline targets microbial protein synthesis and affect the anti-inflammatory response	DB12035
Omadacycline	Bacteria	Omadacycline blocks the 30S ribosomal subunit of bacteria and inhibit protein synthesis.	DB12455
Pentamidine	Protozoa	The mechanism of action is not fully known. It is believed to inhibit DNA, RNA and protein synthesis.	DB00738
Praziquantel	Parasites	Pentamidine acts against parasite worms' muscle by creating muscle contraction with rapid Ca^{2+} influx	DB01058

Table3: Mode of action of shortlisted anti-microbial drugs

Acknowledgements

We thank CSIR and AcSIR for academic support.

References

1. Tan YW, Fang S, Fan H, Lescar J, Liu DX. Amino acid residues critical for RNA-binding in the N-terminal domain of the nucleocapsid protein are essential determinants for the infectivity of coronavirus in cultured cells. *Nucleic Acids Res*. 2006;34(17):4816-4825.
2. Berman HM, Henrick K, Nakamura H (2003). Announcing the worldwide Protein Data Bank. *Nature Structural Biology* 10 (12): 980.
3. Wishart DS, Knox C, Guo AC, Shrivastava S, Hassanali M, Stothard P, Chang Z, Woolsey J (2006). Drugbank: a comprehensive resource for in silico drug discovery and exploration. *Nucleic Acids Research.* (Database issue): D668-72. 16381955.
4. http://mgltools.scripps.edu/downloads
5. Trott O, Olson AJ (2010). AutoDock Vina: Improving the speed and accuracy of docking with a new scoring function, efficient optimization and multithreading, *Journal of Computational Chemistry* 31: 455-461
6. Dassault Systèmes BIOVIA, Discovery Studio Modelling Environment, Release 2017, San Diego: Dassault Systèmes, 2016.
7. DeLano W L (2002). PyMOL. DeLano Scientific, San Carlos.